



## Polyimide-based membrane materials for CO<sub>2</sub> removal from flue gases

Magdalena Wójtowicz, Eugenia Grabiec, Andrzej Jankowski,  
Aleksandra Wolińska-Grabczyk\*

Centre of Polymer and Carbon Materials, Polish Academy of Sciences, 34 M. Curie-Skłodowska, 41-819 Zabrze, Poland, Tel. +48 32 2716077 Ext. 105; Fax: +48 32 2712969; emails: mwojtowicz@cmpw-pan.edu.pl (M. Wójtowicz), egrabiec@cmpw-pan.edu.pl (E. Grabiec); Tel. +48 32 2716077 Ext. 107; Fax: +48 32 2712969; email: ajankowski@cmpw-pan.edu.pl (A. Jankowski); Tel. +48 32 2716077 Ext. 114; Fax: +48 32 2712969; email: awolinska@cmpw-pan.edu.pl (A. Wolińska-Grabczyk)

Received 28 April 2016; Accepted 18 July 2016

### ABSTRACT

This work reports the gas separation properties of polyimides (PIs) with different chemical structures, designed for the removal of carbon dioxide from flue gases. To study the effect of a backbone structure on gas permeability and selectivity, three different methods of chemical modification of the poly(hydroxyimide) (PIOH) were applied. The introduction of bulky pendant groups in a PI chain was accomplished by Mitsunobu reaction; conversion of PIOH to polybenzoxazole rigid structure (PITR) was performed by thermal cyclization in an inert atmosphere, whereas incorporation of CO<sub>2</sub>-philic polyoxyethylene (PEO) segments into main chain was carried out at the polycondensation stage by using a mixture of aromatic and PEO-based diamines. The modified polymers were characterized by nuclear magnetic resonance (1H NMR) and fourier transform infrared (FTIR) spectroscopies, and thermo gravimetric analysis (TGA), differential scanning calorimetry (DSC) and wide-angle X-ray diffraction (WAXD) techniques. It was found that the performed modifications resulted in membrane materials with significantly improved gas permeability and either maintained or even improved CO<sub>2</sub>/N<sub>2</sub> selectivity.

*Keywords:* Polyimides; Gas separation; Membranes

### 1. Introduction

The separation of gases by membranes is a dynamic and rapidly growing field. In terms of economic considerations, it is now recognized as a very significant unit operation able to decrease costs of many industrial processes and to reduce their environmental impact. An area of increasing importance is the capture of carbon dioxide from flue gases generated by the combustion of fossil fuels and other human activities. CO<sub>2</sub> is the main greenhouse gas causing global warming, and the reduction of its emission to the atmosphere is of a major concern [1]. Separation of CO<sub>2</sub> from gas mixtures can be carried out by various conventional methods, including

absorption in amine solutions, adsorption or cryogenic separation. Comparing with those techniques, membrane separation can be much more energy efficient. Moreover, it is compact and easy to scale up, fully automated, and of low capital and operating costs, and it does not need any addition of potentially expensive adsorbents and/or difficult to handle solvents. However, to make this technique more competitive for CO<sub>2</sub> removal from flue gases, new membrane materials with higher permeability and selectivity are required. These materials should also be thermally and chemically stable, resistant to plasticization and physical aging, and have good processability. Currently, polymeric membranes have the largest potential to meet those requirements. Among them, aromatic polyimides (PIs) provide required properties such

\* Corresponding author.

Presented at the conference on Membranes and Membrane Processes in Environmental Protection (MEMPEP 2016), Zakopane, Poland, 15–19 June 2016.

as excellent film-forming ability, easy processability, high thermal stability, good chemical resistance and mechanical durability, and better permeability comparing with many other glassy polymers.

Unfortunately, polymeric membranes, which have high gas permeability, exhibit low selectivity and vice versa. This behavior has been demonstrated by Robeson, who expressed it in a form of an upper bound relationship between the log of the separation factor and the log of the permeability of a faster permeating gas [2]. Thus, the upper bound relationship creates the limit for achieving the desired result of a high separation factor along with a high permeation rate for a given gas pair. Since the first publication concerning the upper bound, a large number of studies have been carried out to exceed this limit. Both Freeman [3] and Alentiev et al. [4] indicated that one way to overcome the upper bound is by enhancing the solubility of the “faster” gas, which in turn should lead to the selectivity and permeability improvement. This approach was used by us for tailoring the PI structure. In the present work, the solubility was planned to be enhanced due to incorporation of CO<sub>2</sub>-philic groups, such as pyridine and ethylene oxide moieties, into a PI chain, or due to the increased PI free volume. The latter strategy, realized by introducing bulky groups or by developing microporosity in PI, should also lead to higher diffusion rates. The aim of these studies was to find correlations between PI structure, modified according to the presented concept, and its gas transport properties. The structure modifications were carried out for PI containing hydroxyl (OH) groups by using Mitsunobu reaction, by thermal rearrangement of *ortho*-OH in the imide moiety, and by copolycondensation reaction to introduce ethylene oxide-based soft segment into PI main chain.

## 2. Experimental part

### 2.1. Polymer synthesis

The PI containing hydroxyl groups, PIOH, was synthesized by the polycondensation reaction of 3,3'-dihydroxybenzidine (HAB) and 4,4'-(4,4'-isopropylidenediphenoxy) bis(phthalic anhydride) (BPADA) performed in a mixture of *N*-methyl-2-pyrrolidone (NMP) and *o*-dichlorobenzene (80/20 [v/v], 20 wt% of the total monomer concentration) according to the method described in [5]. The reaction was carried out in a two-neck flask equipped with an argon gas inlet, a Dean–Stark trap, and a reflux condenser. The Dean–Stark trap was filled with 1 ml of *o*-dichlorobenzene. While continually stirring, the reaction mixture was slowly heated up to 180°C for 3 h and maintained at this temperature for 3.5 h to complete the solution imidization process. Next, the polymer solution was cooled to room temperature and poured into methanol. The crude product was redissolved in tetrahydrofuran (THF), reprecipitated in methanol, and dried under vacuum for several days, at temperature increased stepwise up to 150°C.

The PI modified by Mitsunobu reaction, PI-PMe, was obtained as follows. To solution of PIOH in anhydrous NMP, dry triphenylphosphine (TPP) was added under argon atmosphere. Then, at 0°C, diisopropyl azodicarboxylate (DIAD) was added dropwise. The reaction mixture was brought to room temperature, and subsequently 4-pyridinemethanol

(PMe) dissolved in NMP was added [6]. The reaction mixture was stirred at room temperature for 48 h. Next, solution was poured into methanol, and precipitate was filtered and gradually heated under vacuum up to 150°C.

Thermally rearranged polymer, PITR, was obtained by thermal conversion of PIOH performed in a muffle furnace at argon atmosphere. The membrane was placed between two ceramic plates to avoid deformation during thermal processing. The following protocol was used: the heating was carried out up to 300°C at a rate of 10° min<sup>-1</sup>, and the membrane was kept at this temperature for 1 h, after that the heating was continued up to 400°C at a rate of 5° min<sup>-1</sup>, and this final temperature was maintained for 1/2 h. The sample was then cooled to ambient temperature at a rate of 10° min<sup>-1</sup>.

The segmented copolyimide, coPIOH, was synthesized in the polycondensation reaction of BPADA with a mixture of diamines, HAB and polyoxyethylenediamine (Jeffamine ED-2003) in a molar ratio of 3:1, in NMP under an inert atmosphere (80/20 [v/v], 20 wt% of the total monomer concentration). The reaction was carried out in two steps. The first one, which proceeded for 20 h at continuous stirring, concerned the formation of poly(amic acid). The second step involved the solution imidization process. At this stage, toluene was added, and the reaction mixture was heated up to 180°C and maintained at this temperature for 4 h. After imidization reaction was completed, the polymer solution was cooled to room temperature and used for membrane preparation.

### 2.2. Membrane formation

The polymer solution in *N,N*-dimethylformamide (DMF) (5 wt% solid) was filtered through a 0.5- $\mu$ m filter, cast onto a glass plate, and dried at 50°C for 48 h in a convection oven. Then, the film was placed in a vacuum oven and heated slowly to 150°C with holds at 100°C, 120°C, and 135°C, and finally held at 150°C for 16 h to remove the residual solvent. Thickness of the films, calculated as an average of several thickness measurements, was in the range of 40–60  $\mu$ m. The obtained PI membranes were flexible and transparent yellow with the exception for a PITR membrane, which exhibited darkening of the color as well as reduction in size after thermal conversion.

### 2.3. Characteristics

<sup>1</sup>H nuclear magnetic resonance (NMR) spectra were recorded on an Avance II Ultra Shield Q3 Plus Bruker MT 600 MHz spectrometer using dimethyl sulfoxide (DMSO-*d*<sub>6</sub>) as a solvent and tetramethylsilane (TMS) as the internal standard. The infrared (IR) spectra of polymer films were recorded within the range of 4,000–500 cm<sup>-1</sup> using the ATR-FTIR technique, with a Nicolet 6700 FTIR apparatus (Thermo Scientific, MA, USA). DSC investigations were performed with a TA-DSC 2010 apparatus (TA Instruments, Newcastle, DE, USA) at nitrogen atmosphere, using a heating/cooling rate of 20° min<sup>-1</sup>. The glass transition temperatures (*T*<sub>g</sub>) were taken as the midpoint of the heat capacity step change observed in the second run. TGA were carried out on Q-1500 D thermobalance (Hungary) in the temperature range from 25°C to 800°C, at a heating rate of 10° min<sup>-1</sup> at controlled flux of nitrogen. The X-ray diffraction patterns of the samples were

recorded using Ni-filtered Cu-K $\alpha$  radiation (wavelength  $\lambda = 1.54051 \text{ \AA}$ ) on a wide-angle X-ray HZG-4 diffractometer (Carl Zeiss, Jena, Germany) working in the typical Bragg geometry. Gas permeation measurements were performed at 6 bar transmembrane pressure difference and at 30°C using a constant-pressure/variable-volume apparatus [7]. For the permeation experiments, pure oxygen, nitrogen and carbon dioxide were used, and these gases were measured in the given sequence. The gas permeability,  $P$ , expressed in Barrer units was determined using Eq. (1):

$$P = \frac{q \cdot l}{(p_1 - p_2) A \cdot t} \quad (1)$$

where  $q$  is the amount of permeant ( $\text{cm}^3$  (STP)) passing through the membrane in time  $t$  (s);  $A$  is the effective membrane area ( $\text{cm}^2$ );  $l$  is the membrane thickness (cm); and  $p_1$  and  $p_2$  are the upstream and downstream pressures (cm Hg), respectively. The error of permeability coefficient determination that was associated with this system was in the range of 10%–15%, and it was larger for lower gas permeability. The ideal selectivity ( $\alpha$ ) for gases A and B was calculated from single gas permeation experiments using the following equation:

$$\alpha_{AB} = \frac{P_A}{P_B} \quad (2)$$

### 3. Results and discussion

#### 3.1. Chemical modification of PI

The chemical structure of PIOH is shown in Fig. 1.  $^1\text{H}$  NMR and ATR-FTIR spectra of PIOH exhibiting characteristic imide peaks confirmed the assumed polymer structure and completed conversion of a poly(amic acid) precursor into a PI. The resulting PI bearing phenolic hydroxyl groups was further modified using different methods.

The Mitsunobu reaction allows to incorporate new functional groups directly into the PI backbone (Fig. 2). This reaction proceeds between the aliphatic hydroxyl group and the phenol group of the PI in mild conditions [8]. By changing the reaction time, different degree of PI substitution can be obtained. In this work, PIOH was functionalized using PMe, and the substituted PI with maximum 63% functionalization of the OH groups was investigated. The degree of substitution was determined by  $^1\text{H}$  NMR spectroscopy.

In the synthesized PIOH, hydroxyl groups in *ortho*-position to the imide ring allow for its conversion into the respective TR polymer. The cyclization process, occurring as a result of the thermal treatment, is presented schematically in Fig. 3. As it can be seen from this reaction scheme, the thermal rearrangement of poly(hydroxyimide) to polybenzoxazole is accompanied by the release of carbon dioxide. To investigate the process of PIOH conversion, TGA analysis could be used. In the TGA and DTG profiles of PIOH shown in Fig. 4, two distinct weight losses can be noticed. The first one, seen in the range of 320°C–470°C is related to the removal of  $\text{CO}_2$  due to PITR formation, whereas the second one at around 480°C–650°C corresponds to the degradation of the in situ formed PITR. The weight loss of PIOH at the first

stage was found to correspond to 13% of the initial weight that is in accordance with a theoretical value of 12.56%, calculated assuming the release of two  $\text{CO}_2$  molecules per PI repeat unit. The more detailed studies of PIOH conversion carried out in situ using optical measurements are presented elsewhere [9].

Another approach used in this work was to introduce polyether blocks into the PIOH chain by carrying out a copolymerization of the respective monomers. In Fig. 5, the repeat unit of the segmented coPIOH is schematically given. Due to the thermodynamic incompatibility of both rubbery (SS) and hard glassy (HS) segments, they undergo microphase separation resulting in two-phase morphology. The hard segment domains serve as virtual cross-links for the soft segments as well as reinforcing filler improving PI mechanical

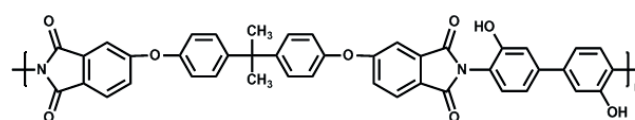


Fig. 1. Structure of PIOH.

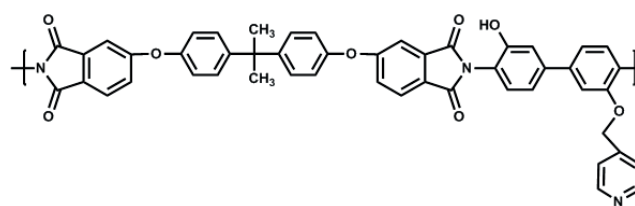


Fig. 2. Structure of PMe substituted PIOH.

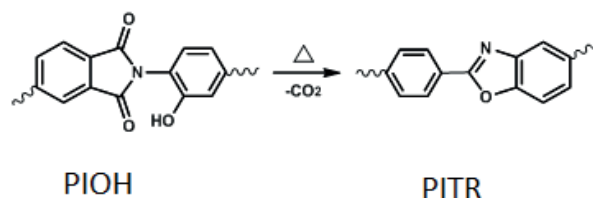


Fig. 3. Schematic representation of PIOH to PITR thermal rearrangement.

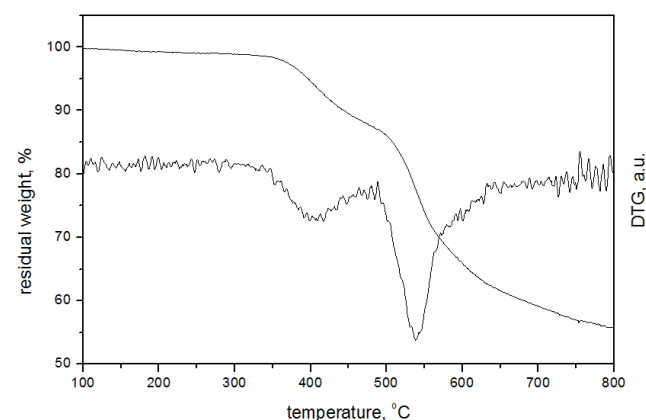


Fig. 4. TGA thermogram of PIOH.

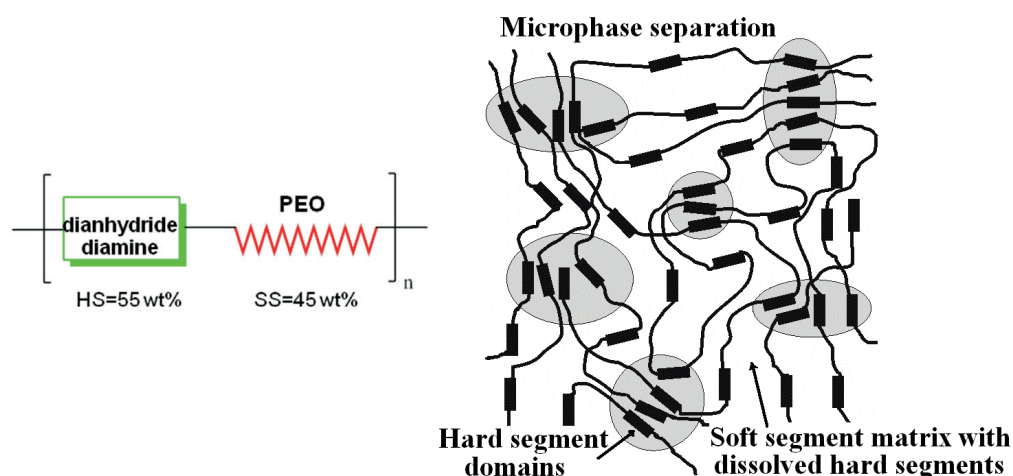


Fig. 5. Schematic representation of coPIOH repeat unit and microphase separation.

Table 1  
Thermal characteristics of PIs

Polymer code	DSC	TGA		
	<sup>a</sup> T <sub>g</sub> (°C)	<sup>b</sup> T <sub>5%</sub> (°C)	<sup>c</sup> T <sub>deg</sub> (°C)	<sup>d</sup> Char yield (wt%)
PIOH	289	382	539	54
PI-PMe	186	242	504	53
PITR	nd*	524	546	62
coPIOH	14 SS 234 HS	331	372 596	2

<sup>a</sup>T<sub>g</sub> – glass transition temperature estimated by DSC, II run by heating 20° deg min<sup>-1</sup>.

<sup>b</sup>T<sub>5%</sub> – temperature at 5% weight loss.

<sup>c</sup>Temperature of maximum decomposition rate.

<sup>d</sup>Residual weight when heated at 650°C in nitrogen.

\*Not detected up to 500°C.

Table 2  
Physical properties of PIs

Polymer code	<i>d</i> -spacing, Å	Density, g cm <sup>-3</sup>
PIOH	4.95	1.285
PI-PMe	4.87	1.252
PITR	5.00	1.229
coPIOH	4.32	1.264

Table 3  
Gas permeation properties of PIs; 30°C

Polymer code	N <sub>2</sub> (Barrer)	O <sub>2</sub> (Barrer)	CO <sub>2</sub> (Barrer)	α <sub>O<sub>2</sub>/N<sub>2</sub></sub>	α <sub>CO<sub>2</sub>/N<sub>2</sub></sub>
PIOH	0.019	0.165	0.67	8.7	35.5
PI-PMe	0.058	0.414	1.74	7.1	30.0
PITR	0.092	0.664	2.55	7.2	27.7
coPIOH	0.023	0.154	1.29	6.6	56.1

properties. Transport of small molecules proceeds through both hard microdomains and elastomeric phase; however, the properties of both phases strongly depend on the degree of microphase separation. If the microphase separation is not complete, hard segment units may be present in the soft segment matrix, as well as some soft segments may dissolve in the hard microdomains modifying their initial transport properties.

### 3.2. Physicochemical and gas transport properties of polyimides

Thermal behavior of the obtained polymers was investigated by DSC and TGA techniques, and the results are given in Table 1.

From these data, it can be seen that for PITR any *T<sub>g</sub>* was detected in the DSC scans, which means that it is probably above the temperature marking the start of PITR degradation. This result indicates that the main chain of PI is converted into a highly stiff backbone structure. As observed for PI-PMe, the introduction of a new moiety to the polymer chain reduces its *T<sub>g</sub>* value by 100°C comparing with that of the PIOH precursor. Segmented coPIOH is characterized by the presence of two *T<sub>g</sub>*'s at 14°C and 234°C. The first one, detected in the subambient temperature range, refers to the soft segment domains, whereas the second *T<sub>g</sub>* found in the high temperature region, concerns the hard segment domains. This result is indicative of a two-phase morphology of coPIOH as shown in Fig. 5. *T<sub>g</sub>* of coPIOH hard domains is lower than that of PIOH being its fully aromatic analogue, what suggests some mixing of soft segments into hard domains. Similarly, *T<sub>g</sub>* of the soft matrix is much higher than that of polyoxyethylenediamine (*T<sub>g</sub>* estimated at -58°C) pointing at a substantial amount of hard segments being incorporated into soft matrix. From the data in Table 1, it is also seen that PITR displays the highest thermal resistance among the other PIs studied. The beginning of its degradation (*T<sub>5%</sub>*) falls at temperature by 140°C higher than that of its precursor, and by 280°C higher than that of the functionalized PI. For coPIOH, two-stage degradation was observed. The first stage comprises degradation of the polyether-based soft segments, whereas the second one, taking place at higher temperature, refers to the degradation of the aromatic hard segments.

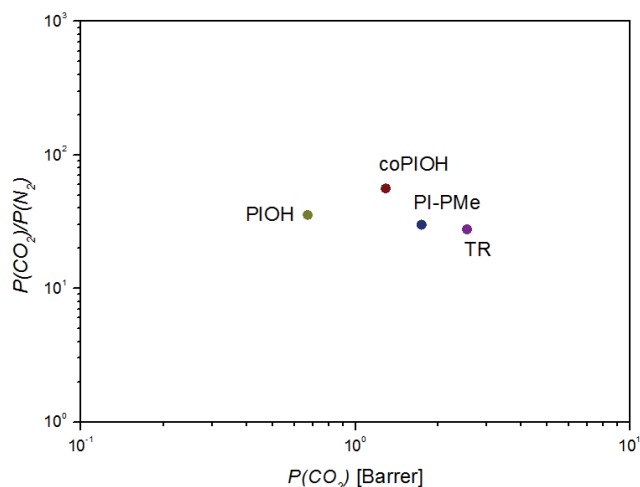


Fig. 6. The upper bound correlation for  $\text{CO}_2/\text{N}_2$  gas pair.

Wide-angle X-ray diffraction (WAXD) method was used to characterize morphology of the studied polymer films. These samples show a broad halo in the diffraction curve indicating amorphous character of PIs. The  $d$ -spacing values calculated from the position of the halo maxima and the measured densities of the studied PIs are presented in Table 2.

It can be noticed that the intermolecular distances represented by the  $d$ -spacing values are very similar for all the aromatic PIs studied. In contrary, segmented coPIOH shows a significantly reduced value of the  $d$ -spacing. This can be attributed to the presence of the flexible PEO segments allowing the PI segments to pack more efficiently. This explanation is also supported by only a slightly reduced density value of coPIOH comparing with its fully aromatic analogue. On the other hand, for both modified aromatic PIs, the measured densities are significantly lower than for their PIOH precursor. This indicates that both thermal transformation of a PIOH main chain and its functionalization caused the disruption of chains packing.

Gas permeation data obtained for the investigated polymers are gathered in Table 3 and presented in a Robeson diagram in Fig. 6. Based on the data, it can be found that the transformations of PIOH to PI-PMe, PITR and coPIOH all lead to the improvement in gas transport properties. Thermal rearrangement causes the highest increase in permeability. For PITR, fivefold and fourfold permeability enhancement was observed for  $\text{N}_2$  and  $\text{CO}_2$ , respectively. In this case, the obtained  $\text{CO}_2/\text{N}_2$  ideal selectivity was slightly reduced comparing with that of PIOH. On the other hand, approximately, threefold increase in the  $P$  value was noticed for PI-PMe comparing with PIOH. Similarly, the enhancement in PI-PMe permeability was accompanied by a slight drop in  $\text{CO}_2/\text{N}_2$  ideal selectivity. In contrary, for coPIOH, the permeability increase was only observed for  $\text{CO}_2$ . As a result, a significant increase in  $\text{CO}_2/\text{N}_2$  selectivity was obtained (Fig. 6).

#### 4. Final remarks

Three different methods of chemical modification of PIOH structure were used with the aim of studying their effect on gas transport properties of the resulting membranes. It was

demonstrated that all those methods allowed to obtain membranes with better transport characteristics. Permeabilities of the gas penetrants through the modified, fully aromatic PIs were enhanced over the permeability of the PIOH precursor. The highest permeability improvement was noticed for the thermally rearranged PI. Moreover, the permeability increase was generally associated with only a slight decline in  $\text{CO}_2/\text{N}_2$  ideal selectivity for those PIs. In contrast, the segmented coPIOH exhibited a marked increase in both  $\text{CO}_2$  permeability and  $\text{CO}_2/\text{N}_2$  ideal selectivity. The relatively high permeability and selectivity of this copolymer could be attributed to the strong interaction between  $\text{CO}_2$  molecules and polyoxyethylene-based soft segments, which increased  $\text{CO}_2$  solubility in the membrane allowing the Robeson correlation to be overcome.

#### Symbols

$P, P_A, P_B$	—	Permeability coefficient, Barrer
$\alpha$	—	Ideal selectivity
$q$	—	Permeate volume, $\text{cm}^3$ (STP)
$l$	—	Membrane thickness, cm
$p_1, p_2$	—	Feed, permeate pressure, cm Hg
$A$	—	Effective membrane area, $\text{cm}^2$
$t$	—	Time, s

#### Acknowledgment

This research was supported by the DoktoRIS project – scholarship program for the innovation of Silesia region supported by the European Community from the European Social Fund.

#### References

- [1] Z. Zhang, J. Sunarso, S. Liu, R. Wang, Current status and development of membranes for  $\text{CO}_2/\text{CH}_4$  separation: a review, *Int. J. Greenhouse Gas Control*, 12 (2013) 84–107.
- [2] L.M. Robeson, Correlation of separation factor versus permeability for polymeric membranes, *J. Membr. Sci.*, 62 (1991) 165–185.
- [3] B.D. Freeman, Basis of permeability/selectivity tradeoff relations in polymeric gas separation membranes, *Macromolecules*, 32 (1999) 375–380.
- [4] A. Alentiev, Y. Yampolskii, J. Kostina, G. Bondarenko, New possibilities for increasing the selectivity of polymer gas separating membranes, *Desalination*, 199 (2006) 121–123.
- [5] H.-J. Lee, M.-H. Lee, S.G. Han, H.-Y. Kim, J.-H. Ahn, E.-M. Lee, Y.H. Won, Synthesis and properties of nonlinear optical side chain soluble polyimides for photonics applications, *J. Polym. Sci. A Polym. Chem.*, 36 (1998) 301–307.
- [6] S. Park, K. Kim, J.C. Kim, W. Kwon, D.M. Kim, M. Ree, Synthesis and nonvolatile memory characteristics of thermally, dimensionally and chemically stable polyimides, *Polymer*, 52 (2011) 2170–2179.
- [7] A. Wolińska-Grabczyk, A. Jankowski, R. Sekuła, B. Kruczek, Separation of  $\text{SF}_6$  from binary mixtures with  $\text{N}_2$  using commercial poly(4-methyl-1-pentene) films, *Sep. Sci. Technol.*, 45 (2011) 1231–1240.
- [8] K.C.K. Swamy, N.N.B. Kumar, E. Balaraman, K.V.P.P. Kumar, Mitsunobu and related reactions: advances and applications, *Chem. Rev.*, 109 (2009) 2551–2651.
- [9] B. Jarzabek, M. Wójtowicz, A. Wolińska-Grabczyk, Optical studies of poly(hydroxy imide) to polybenzoxazole thermal rearrangement, *Macromol. Chem. Phys.*, 216 (2015) 2377–2385.